

## 9.8 Application and issues of SZ phase coding for NEXRAD

J.C. Hubbert,\* G. Meymaris, S. Ellis and M. Dixon  
National Center for Atmospheric Research, Boulder CO

### 1. INTRODUCTION

SZ phase coding has proved to be an effective technique to mitigate the range-velocity ambiguity problem for weather radars. NCAR and NSSL (National Severe Storms laboratory) have delivered a SZ algorithm that will be deployed on the NWS's (National Weather Service) NEXRAD network of radars when the NEXRADs are updated with the new RDA (Radar Data Acquisition) which is the RVP8 from SIGMET. The SZ algorithm to be employed by the NEXRADs uses spectral processing on contiguous blocks of length 64 time series (i.e., the I and Q samples). The NWS is also pursuing so called "Super Resolution Data". It is desired to increase azimuthal resolution from 1 degree to 1/2 degree. If one degree resolution was accomplished by integrating over 64 points, then Super Resolution would be achieved by simply integrating over 32 points. This then presents a problem for the compatibility of the SZ algorithm and Super Resolution data. This paper examines this and shows hows using overlapping "windows" of time series data alleviates the problem. The idea of overlapping windows can also be used to improve the new spectral clutter filter, GMAP, to be used by the NEXRADs.

### 2. BACKGROUND

Weather radars that use equi-spaced transmit pulse trains to illuminate the atmosphere have limited unambiguous range and unambiguous velocity that depend upon the used PRT (pulse repetition interval). This limitation is succinctly described by the equation  $r_a v_a = c\lambda/8$  where  $r_a$ ,  $v_a$  are the unambiguous range and velocity, respectively, for wavelength  $\lambda$  and where  $c$  is the speed of light. Since the product  $r_a v_a$  is constant for a particular wavelength, increasing either one ( $r_a$  or  $v_a$ ) necessarily decreases the other. At S-band for a PRT of one millisec., the unambiguous range is 150 km while the unambiguous velocity is 25 m/s. Weather phenomena routinely exceed these limits which can result in poor data quality, i.e., folded velocity estimates and range folded echoes. It has been shown that SZ(8/64) phase coding of the transmitted radar pulses is an effective way to extend the unambiguous range without decreasing the unambiguous velocity (see Sachidananda and Zrnić 1999 for details). This phase coding technique will be used on the new NEXRAD RDA.

The SZ phase coding algorithm requires the use of a

fairly aggressive time series window such as the Hanning or Blackman (Proakis and Manolakis 1988). This is done to reduce the spread the power of the strong trip signal across the velocity spectrum. Also, the window is typically applied to non overlapping contiguous 64 point time series data. In this case, the radar scan rate and sample rate is adjusted so that there are 64 points per resolution volume. What can be done, then, if there are fewer than the required 64 points per resolution volume for SZ phase coding? One approached is to adjust the SZ algorithm to use only 32 points, i.e., SZ(4/32) could be employed. However, since fewer data points are used there is less "information" for the SZ algorithm and as a result the recovered signal statistics are reduced which means poorer data quality. Another approach is to use a sliding overlapping window function. This paper investigates the use of such an overlapping windowing strategy and compares the results to SZ(4/32). Also examined are the statistics of the SZ(4/32), SZ(8/64) and SZ(16/128) algorithms. Data from KOUN, NSSL's (National Severe Storm Laboratory) research radar are used to illustrate some of the theoretical concepts.

### 3. WINDOW FUNCTIONS

In this section the Rectangular, Hanning and Blackman window functions are compared. Mathematically they are defined as,

Rectan.	1 for $0 \leq n < M$ ; 0 otherwise
Hanning	$0.5[1 - \cos(\frac{2\pi n}{M-1})]$
Blackman	$0.42 - 0.5 \cos(\frac{2\pi n}{M-1}) + 0.08 \cos(\frac{4\pi n}{M-1})$

Figure 1 shows plots of the window functions for for  $M=64$ . As can be seen when applying the Hanning or Blackman window to a time series, the magnitude of time series members are reduced and thus some signal power is lost. In fact the begin and end segments of the time series contribute very little to the power of the signal. Also shown in Fig. 1 is the window functions divided into three region: 1) the first 16 points, labeled P1, 2) the middle 32 points, labeled P2 and the last 16 points, labeled P3. We define:  $P_R$  as the total power under the rectangular curve, i.e.,  $P_R = 64 P_w$  as the total power of a window function  $P_1$ ,  $P_2$ ,  $P_3$  as the power of a window function in the first 16, middle 32 and last 16 points, respectively.

Table 1 shows some interesting power ratios. The first column shows the ratio of the total power of a window

\*EOL/NCAR, Boulder, Colorado 80307, email: hubbert@ucar.edu

WINDOW	$P_w/P_R$	$P_2/(P_1 + P_2 + P_3)$
Rectangular	100%	50%
Hanning	38.1%	91.9%
Blackman	30%	97%

Table 1: *Ratios of window function powers corresponding to Fig. 1.*

to the power in the Rectangular window. The Hanning and Blackman windows contain 38.1% and 30% of the power of the rectangular window respectively, which corresponds to 4.19 dB and 5.23 dB reductions in power. Thus when using these windows on time series, power estimates must be compensated by these reduction factors. The second column shows the power ratio of the middle 32 points of a window to the total power in a window. For Hanning and Blackman windows this ratio is 91.9% and 97%, respectively. Thus, the middle 32 points of a 64 point time series contains a very large majority of the total power in the windowed time series. Taking 10log of these ratios yields -0.37 dB and -0.13 dB (assuming equal distributed power across the time series)! Thus, even if we neglected the power in the  $P_1$  and  $P_2$  areas, the bias of the calculated power would be less than a half of a dB. This then suggests using sliding, overlapping windows for SZ phase coding.

Figure 2 illustrates the overlapping window strategy. Shown are time series samples that are gathered along a particular range ring. The top portion of Fig.2 shows the traditional 64 point windowing strategy, i.e., contiguous non overlapping windows. Each 64 point window corresponds to a radar resolution bin. The bottom portion of Fig.2 shows the overlapping window strategy. The center of the 64 point window is advanced only 32 points each time. The number in parenthesis corresponds to the consecutive windows. In the overlapping strategy, twice the number resolution bins (referred to as “Super Resolution” data) will be created thus increasing the resolution of the processed radar data without smearing the data significantly. Figure 3 gives an alternative depiction of the overlapping windowing strategy. Shown in Fig. 3a are contiguous non overlapping windows versus time or azimuth angle for some radar range. Figure 3b shows the same time series windows that are moved closer together so that there is now an overlap of time series data points. In this way SZ phase coding can be made compatible with Super Resolution data.

Super Resolution could also be made compatible with SZ phase coding by converting the SZ(8/64) phase coding scheme to a SZ(4/32) scheme, i.e., only length 32 time series could be used in the algorithm. This would, however, result in inferior statistics of the recovered radar moments as is shown below. Next we compare the statistics of the SZ(8/64) algorithm to the SZ(4/32) and SZ(16/128) algorithms.

### 3. SZ STATISTICS

The recovery statistics for the weak trip velocity has been shown in Sachidananda and Zrnić (1999). The standard deviation of the recovered weak trip velocity ( $V_2$ ) is calculated as a function of the ratio of the strong to weak trip power ( $P_1/P - 2$ ) and of the spectrum width of the strong trip ( $W_1$ ) using the weak trip spectrum width ( $W_2$ ) as a parameter. The statistics are compiled using simulated data as was done in Sachidananda and Zrnić (1999). Shown in Figs. 4, 5 and 6 is the standard deviation of  $V_1$  for SZ(4/32), SZ(8/64) and SZ(16/128), respectively. As the sequence length increases, the standard deviation of  $V_1$  decreases as expected. The benefit of using as long a sequence length as possible is clearly seen. Shown in Figs. 7, 8 and 9 is the standard deviation of  $V_2$  for SZ(4/32), SZ(8/64) and SZ(16/128), respectively, for weak trip spectrum widths of 3.75 to 4.25  $\text{ms}^{-1}$ . In this case since  $V_2$  is a SZ recovered moment ( $V_1$  is calculated directly from the time series before any SZ processing) and is affected by spectral overlap from the strong trip as well as the overlap of the weak trip replica spectra (see Sachidananda and Zrnić 1999 for details), the effects of lengthening the time series sequence is less certain. Figures 7, 8 and 9, however, again clearly show the reduction of standard deviation of  $V_2$  as the sequence length increases. The result is a significantly extended region of acceptable  $V_2$  recovery, i.e., the recovery region is increased to higher  $P_1/P_2$  power ratios, wider  $W_1$  spectrum widths and wider  $W_2$  spectrum widths for a constant acceptable level of  $V_2$  standard deviation. Thus again, this demonstrates the advantage of using as long a times series as possible. In the case of Super Resolution data and SZ phase coding, using overlapping length 64 windows is clearly superior to using non overlapping length 32 time series sequences.

We next illustrate the use of the overlapping window strategy using data gathered with KOUN, NSSL’s research radar.

### 4. DATA EXAMPLES

The following data was gathered by KOUN on 3 May 1999 in times series format without phase coding. Via post processing, two PPIs are phase coded for first and second trip and then overlaid. The combined data set then can be processed using the SZ recovery algorithm. The advantage of this technique is two fold; 1) experimental data is used 2) the SZ recovered moments can be compared to the original non overlaid data moments. Shown in Fig. 10 are two concatenated power (unitless) PPI scans. The border between the two PPIs is seen at about (-65 km, -55 km). The PPIs are phase coded for first and second trip and then overlaid and combined into one PPI scan. We next focus our attention on the features at about (-40km, -10 km) where there are some sharp power gradients.

Shown in Fig. 11 are zoomed in power PPIs of Fig. 10 that illustrate Super Resolution data. No phase coding is applied, a non overlapping rectangular window is used

and the individual PPIs are not overlaid. Fig. 11a shows the power calculated over 64 points in the conventional manner. Fig. 11b shows power calculated from 32 points (i.e., double the resolution). Indeed the hook echo does have more detail and forecasters would like to have such data. But if phase coding is to be used in conjunction with Super Resolution data, then only 32 point are available if non overlapping windows are used. In other words,  $SZ(4/32)$  would be used but that would degrade signal statistics significantly. Fig. 12 shows the velocity plots that accompany the power plots of Fig. 11. Some folding is evident but again the Super Resolution plot (Fig. 12b) offers more storm detail.

Next we examine the possible smearing effect of using overlapping windows on the data where again no phase coding is used. Fig. 13 shows power when a 64 point Hanning window is used sliding 32 point for each resolution bin, i.e., the resolution is comparable to Fig. 11b. Fig. 14 show the same as Fig. 13 except a Blackman window is used. As can be seen, Figs. 13, and 14 are very similar to the 32 point Super Resolution data of Fig. 11b. Looking closely at regions of highest power gradient does show that there is some smearing of the data but it appears to be minimal at least for this case. Also the smearing appears to be slightly less for the Blackman window of Fig. 14 as compared to the Hanning window of Fig. 13.

The concatenated PPI scans of Fig. 10 are now phase coded, overlaid and separated via the SZ algorithm. Results are compared to the moments calculated from the non overlaid data. First Fig. 15 shows the ratio of first trip power to second trip power for the same region as Figs. 11 to 14. The entire area displayed in Fig. 11-15 lies in the first trip region. The red areas are strong trip regions and the green areas are weak trip regions. As can be seen the power ratios vary considerable over the PPI of Fig. 15. Fig. 16 shows SZ recovered power when using a 64 point Hanning window centered every 32 point, i.e., it slides 32 point per each new resolution bin. Comparing Fig. 16 to the Super Resolution data of Fig. 13, it is difficult to discern visually any degradation of the data.

Figure 17 shows the velocity that accompanies Fig. 16. Comparing Fig. 17 with Fig. 11a it is seen that the variance in the velocity field is greater (i.e., Fig. 17 looks “noisier” than Fig. 11a.). This is to be expected since the process of separating the strong and weak trip moments with phase coding will increase the variance of the recovered velocity. However, now compare Figs. 18 and Fig. 11a to Fig. 17. Fig. 18 shows the 32 point SZ recovered velocity and it displays more variance than the sliding 64 point data of Fig. 17 as expected.

## 5. IMPLICATIONS FOR OVERLAPPING WINDOWS

The use of overlapping windows will increase data quality in several ways. As shown above the use of overlapping Hanning or Blackman windows minimally smears the data. Currently the SZ algorithm slated to be deployed on the NEXRAD network will use

non overlapping 64 point Hanning windows. Instead overlapping 128 point Hanning windows could be used. The resulting data will be smeared minimally but the recovered SZ signal statistics will increase significantly. More velocity data should be recoverable with reduced variance. For example comparing Fig. 18 to Fig. 17 which shows a 32 point SZ recovered velocity and a 64 point SZ recovered velocity. The variance of the 64 point SZ recovered velocity is significantly less. Using a 128 point SZ algorithm instead of a 64 point SZ algorithm will also significantly improve clutter rejection. This has been shown by Ice et al. 2004. At low elevations angles a long PRT scan will precede a short PRT SZ phase coded scan. The long PRT scan has approximately 16 data point per resolution bin. GMAP, the new spectral based clutter filter to be used on the new NEXRAD ORDA, requires the use of a Blackman window. The window uses non overlapping data. Instead the window length should be increased to 32 points and overlapping windows used. This would improve the clutter rejection performance of the GMAP filter.

## 6. CONCLUSIONS

SZ phase coding of of radar transmitted pulses has been shown to be an effective method to mitigate range-velocity ambiguities. Application of the decoding algorithm requires the use of a Hanning time series window or the equivalent. When using such window functions it was shown that the large majority of the measure power results from the middle half of the windowed points. Thus, instead of applying the window to non overlapping time series points, it was shown that overlapping windows could be used to either 1) increase the resolution of the data or 2) increase the window length to improve SZ recovered moment statistics. Using overlapping windows make doubling the resolution of the radar data possible when using SZ phase coding. Also by using increase length windows, clutter filters, such as GMAP, will have better performance.

**Acknowledgment** This research was supported by the ROC (Radar Operations Center) of Norman OK.

## References

- Ice, R.L., R. Rhoton, D. Saxion, N. Patel, S. Sirmans, D. Warde, D. Rachel and R. Fehlen, 2004: ROC Evaluation of the WSR-88D ORDA System Signal Processing, 20<sup>th</sup> Conf. on IIPS, AMS Annual Meeting, San Diego, CA.
- Proakis, J.G. and D.G. Manolakis, 1988: Introduction to Digital Signal Processing, Macmillan Publishing Co., New York.
- Sachidananda, M. and D.S. Zrnić, 1999: Systematic Phase Codes for Resolving Range overlaid Signals in a Doppler Weather Radar *JTECH*, **16**, 1351-1363.

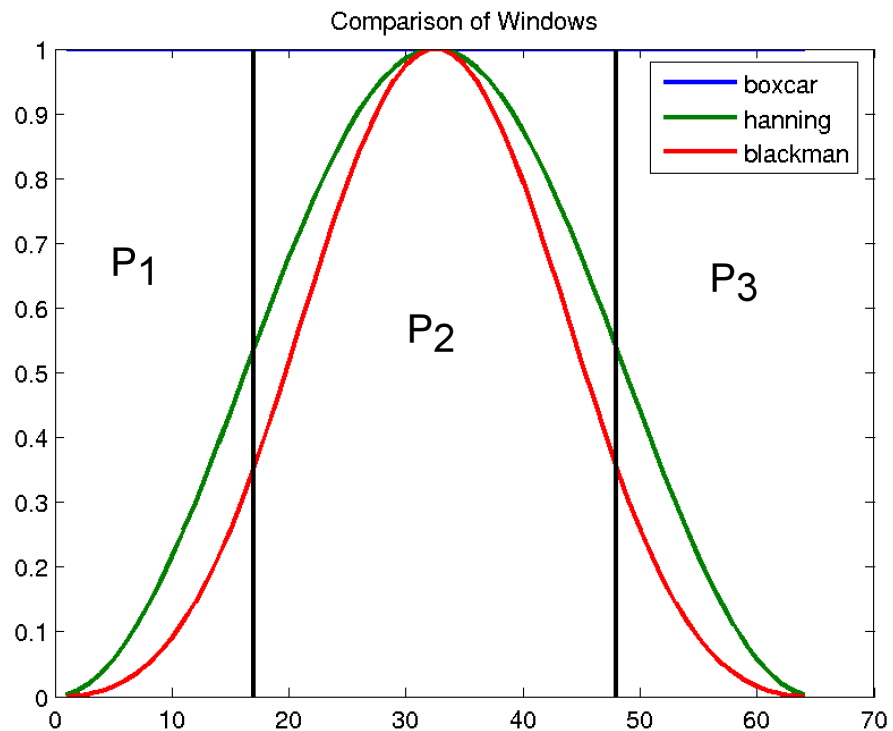
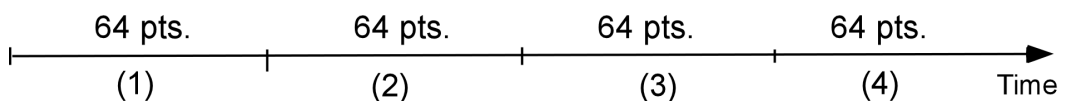
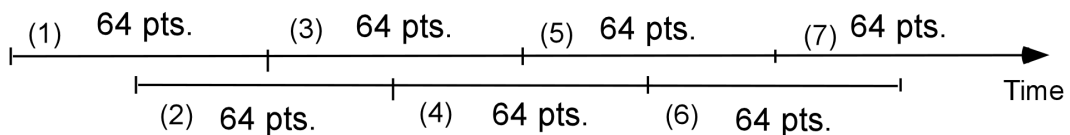


Figure 1: *Window functions.*



Typical integration strategy: non overlapping time series



## Sliding window sampling strategy: overlapping time series

Figure 2: *Overlapping window strategy.*

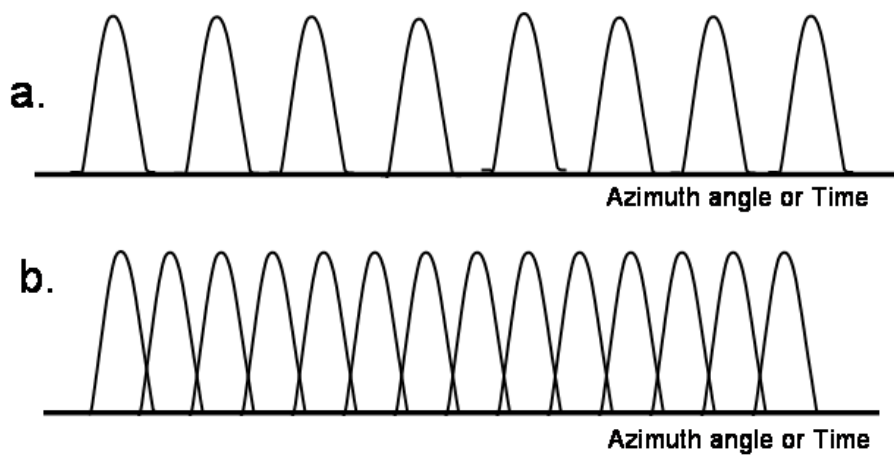


Figure 3: *Schematic of non overlapping time series windows (a.) and overlapping time series windows. Panel (a.) depicts “normal resolution” while Panel (b.) depicts windowing for Super Resolution data.*

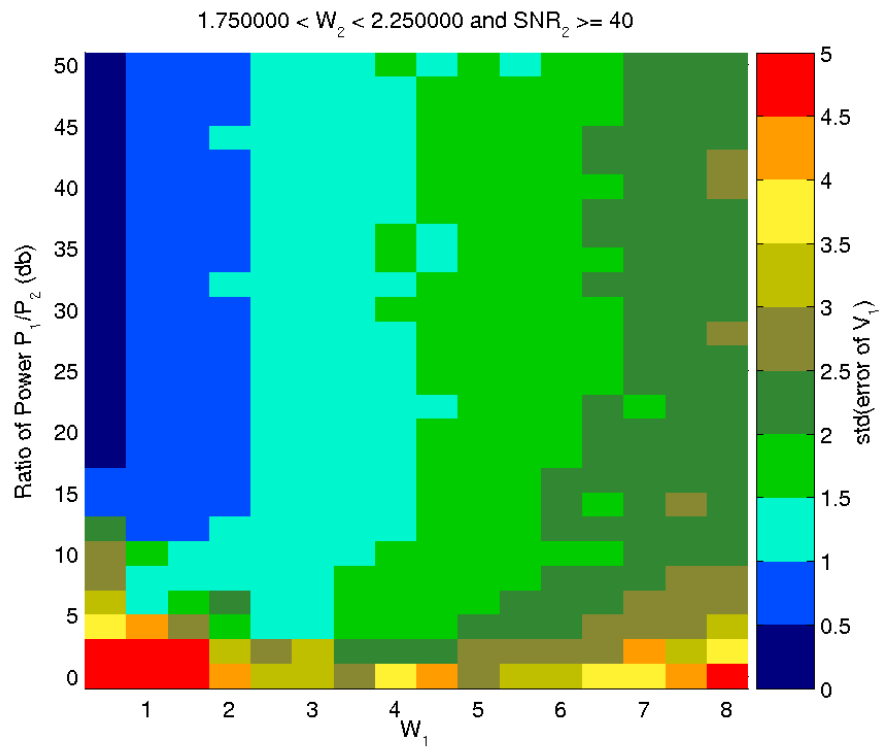


Figure 4: The standard deviation of strong trip velocity for  $SZ(4/32)$  algorithm.

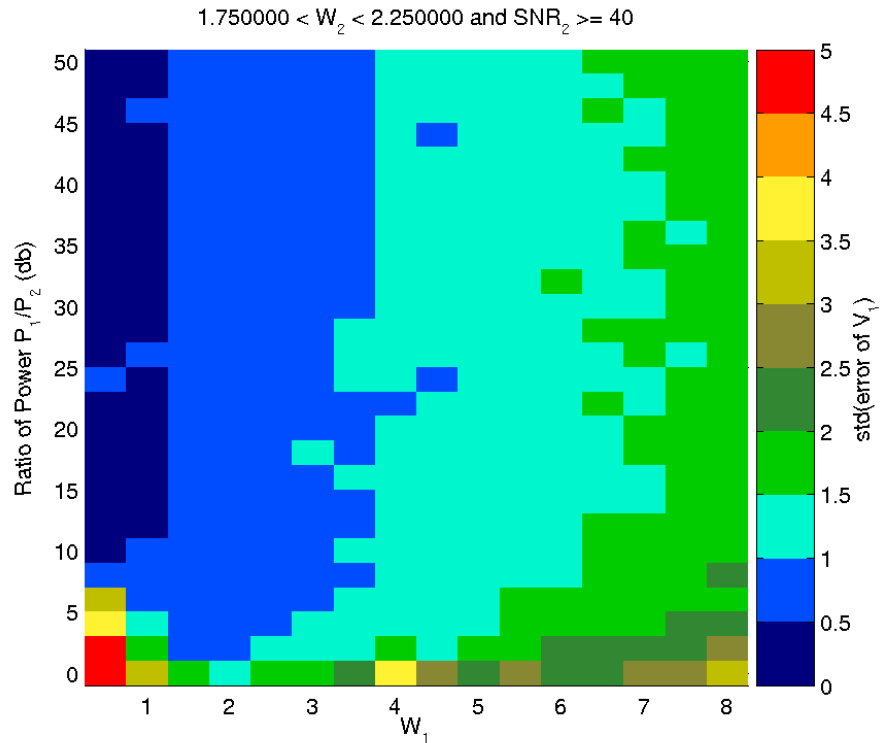


Figure 5: The standard deviation of strong trip velocity for  $SZ(8/64)$  algorithm.

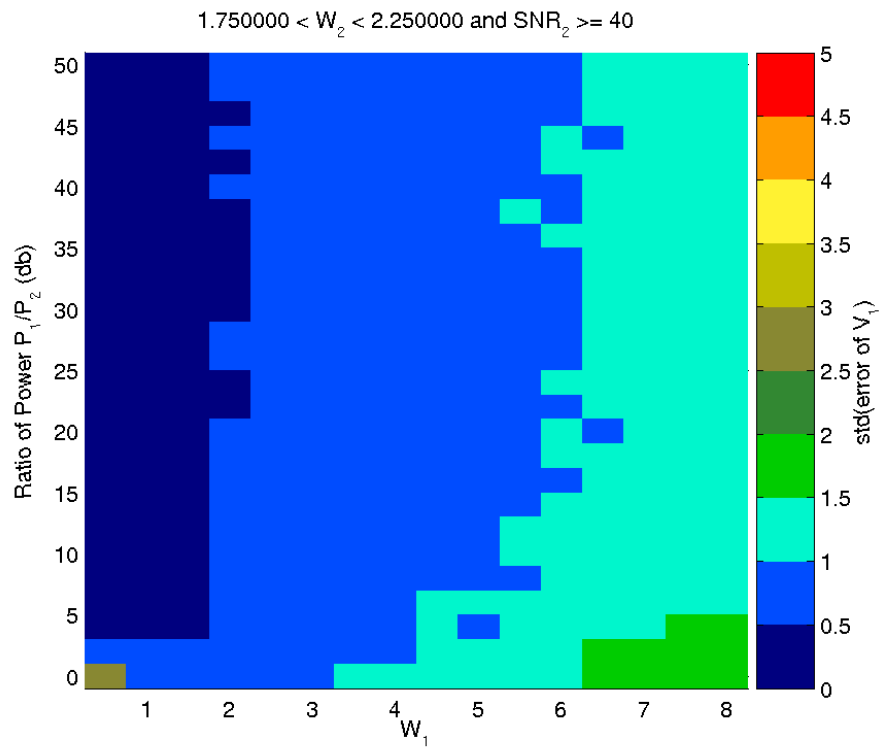


Figure 6: The standard deviation of strong trip velocity for  $SZ(16/128)$  algorithm.

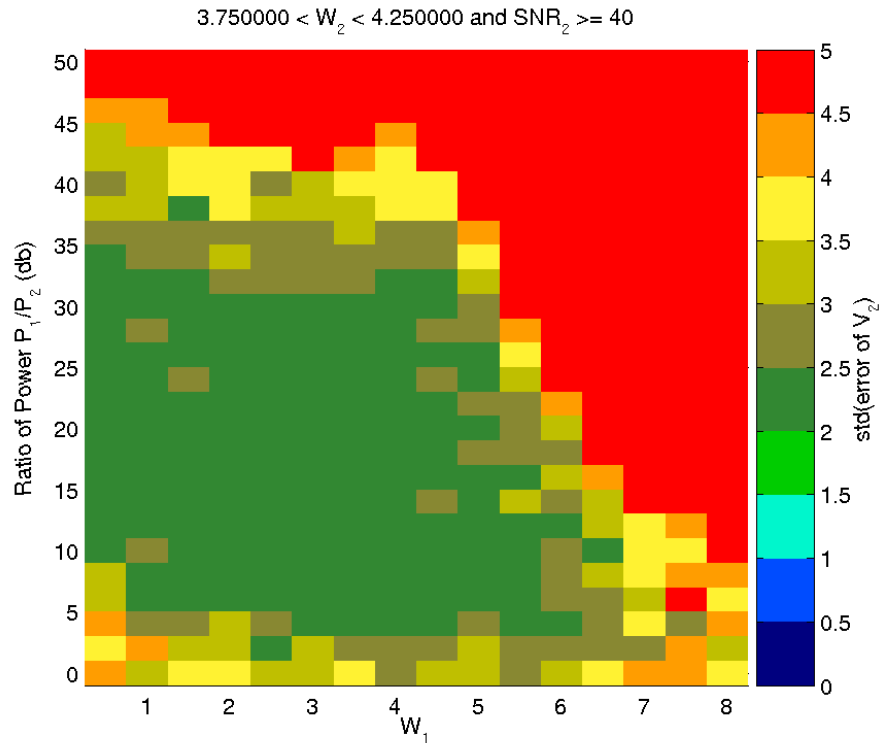


Figure 7: The standard deviation of weak trip velocity for  $SZ(4/32)$  algorithm.

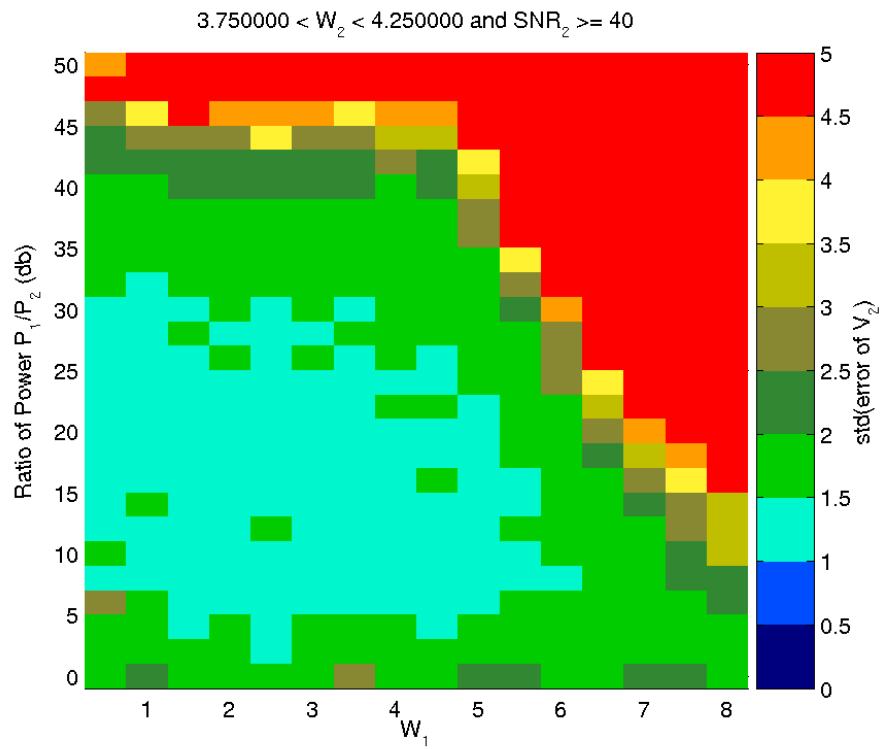


Figure 8: The standard deviation of weak trip velocity for SZ(8/64) algorithm.

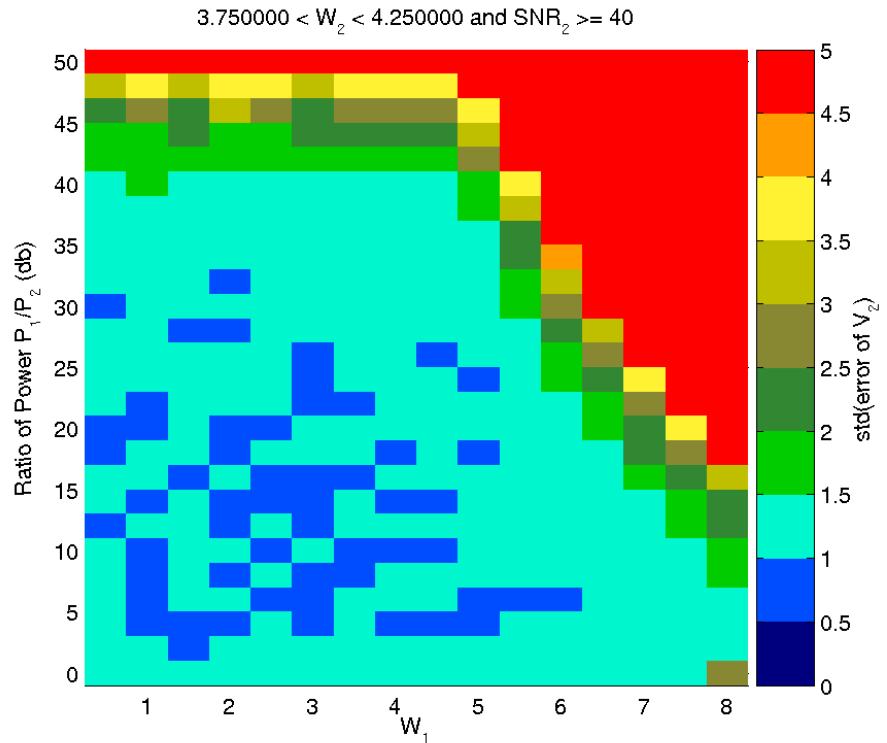


Figure 9: The standard deviation of weak trip velocity for SZ(16/128) algorithm.

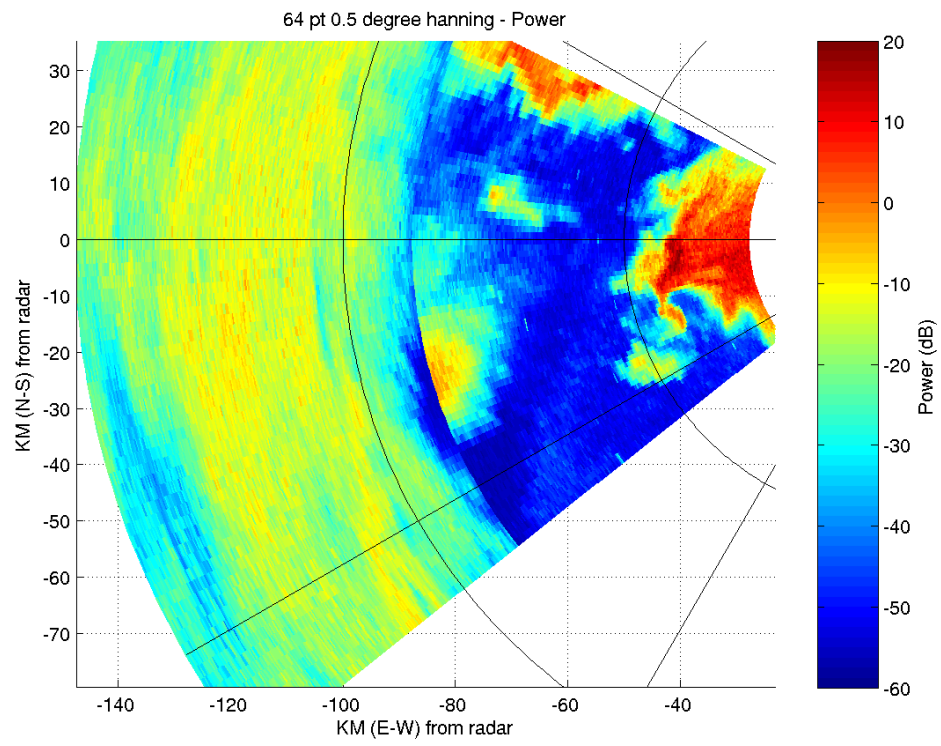


Figure 10: *Concatenated power PPI scans.*

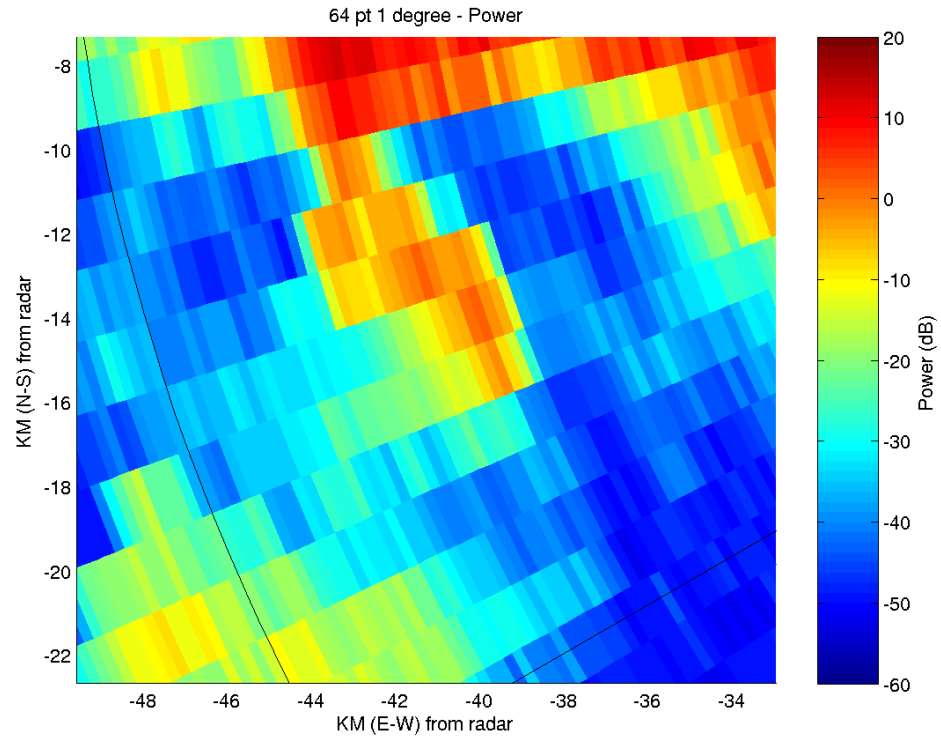


Figure 11a: *Close up of Fig. 10. Power is calculated over non overlapping 64 point windows.*

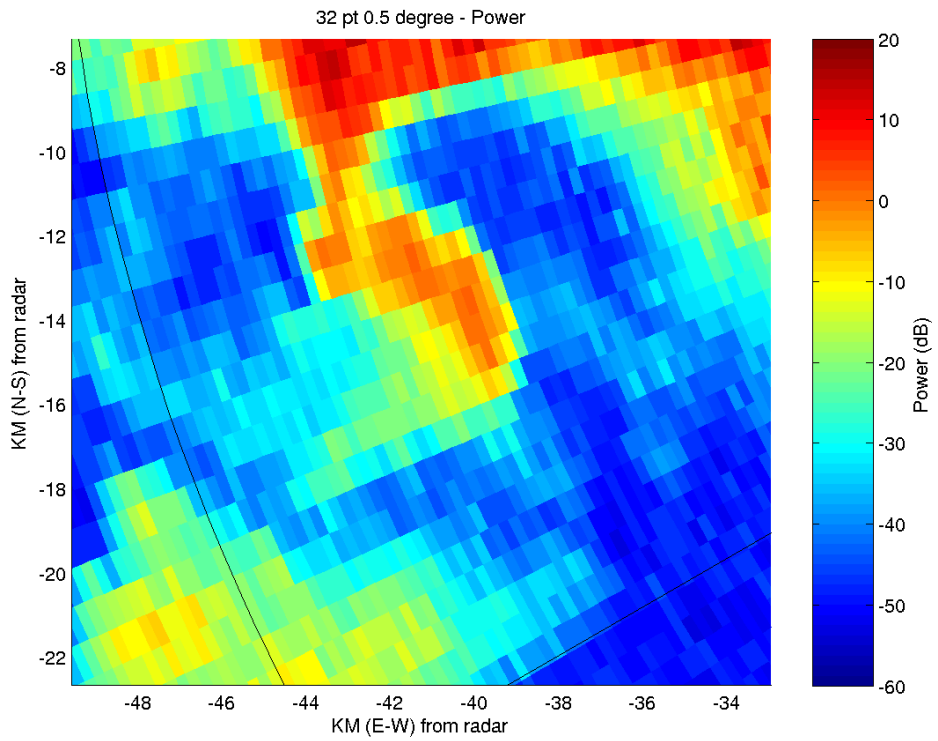


Figure 11b: *Super resolution data, i.e., power is integrated over 32 points.*

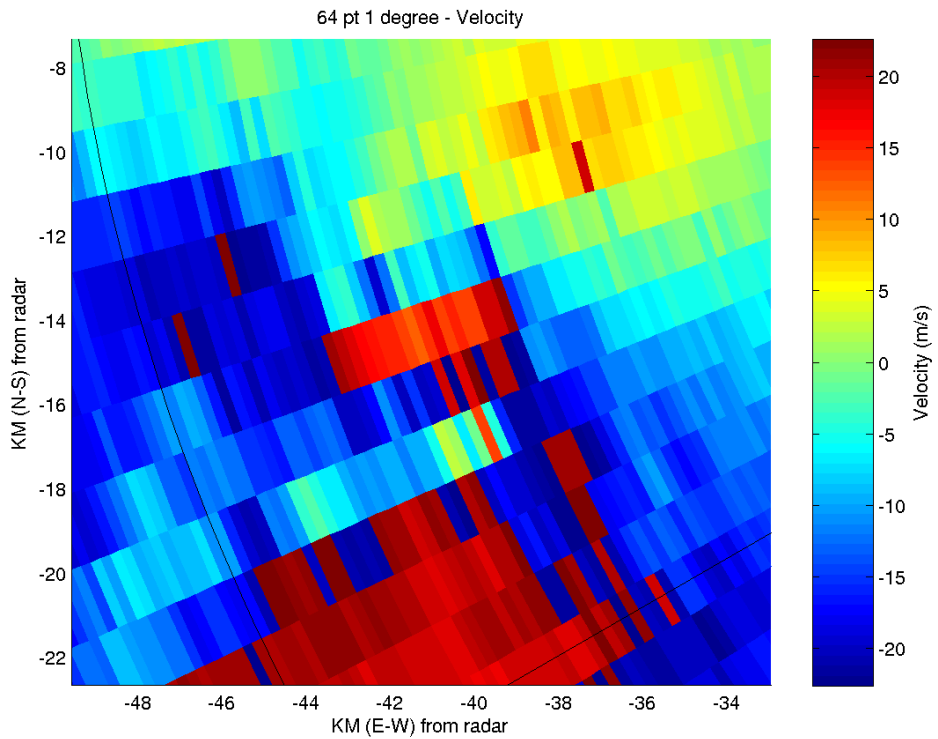


Figure 12a: *Velocity accompanying Fig. 11a.*

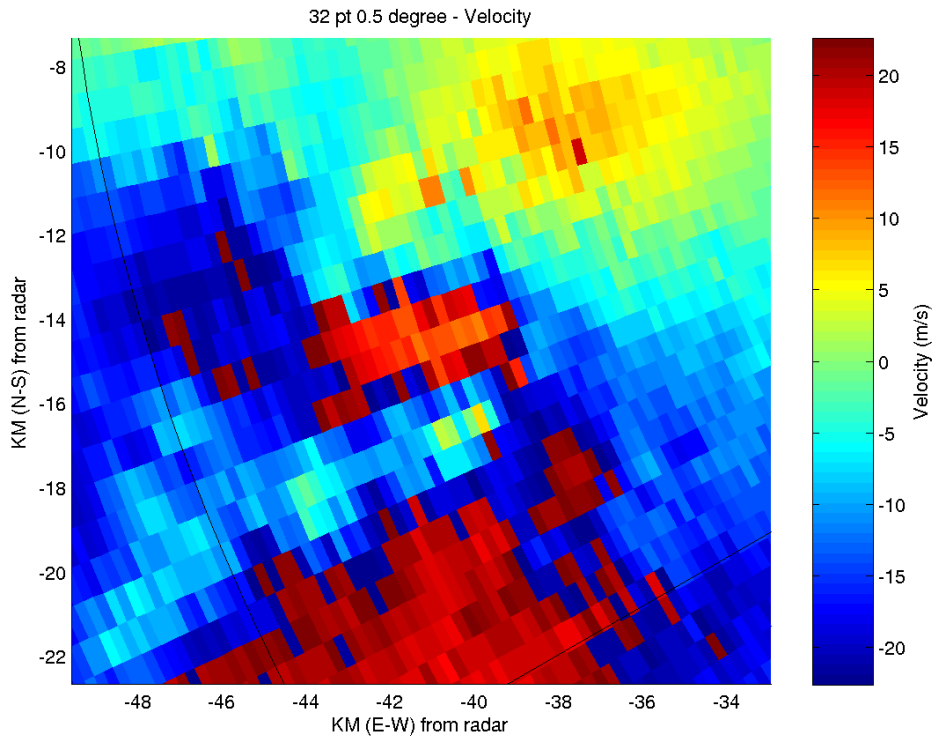


Figure 12b: *Super resolution velocity accompanying Fig. 11b.*

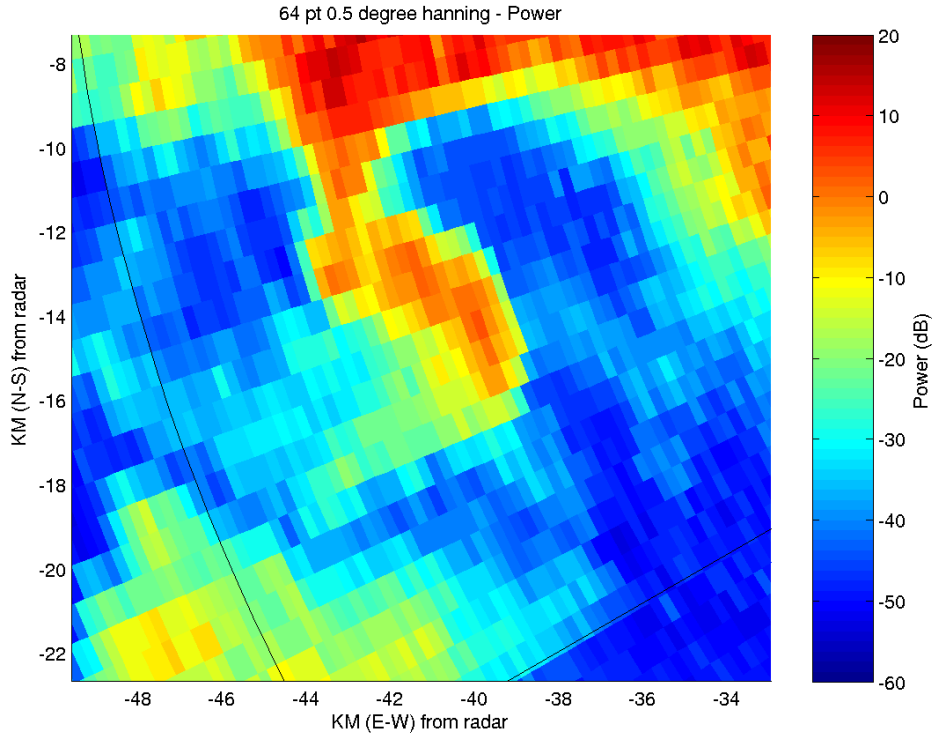


Figure 13: *Power calculated over 64 point Hanning window but at 32 point intervals. No phase coding is applied.*

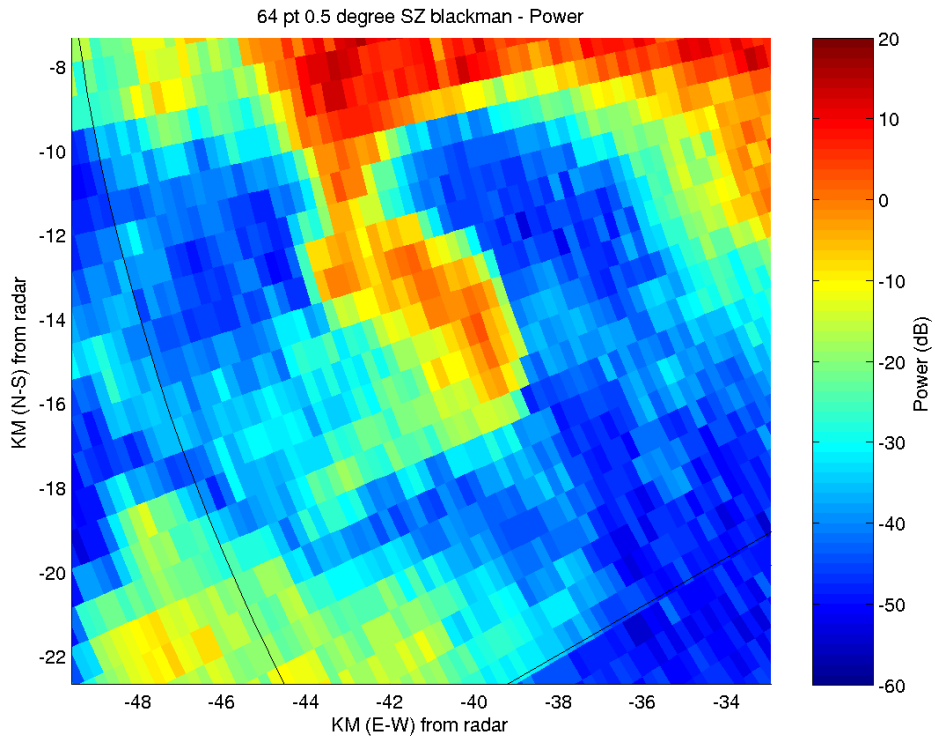


Figure 14: Power calculated over 64 point Blackman window but at 32 point intervals. No phase coding is applied.

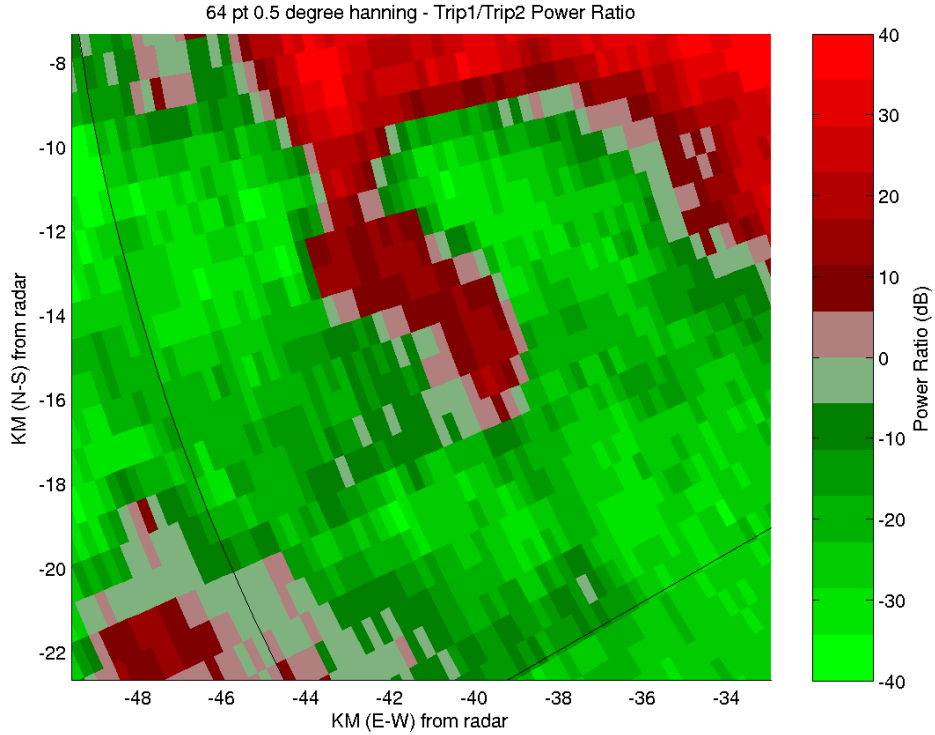


Figure 15: Ratio of first trip power to second trip power.

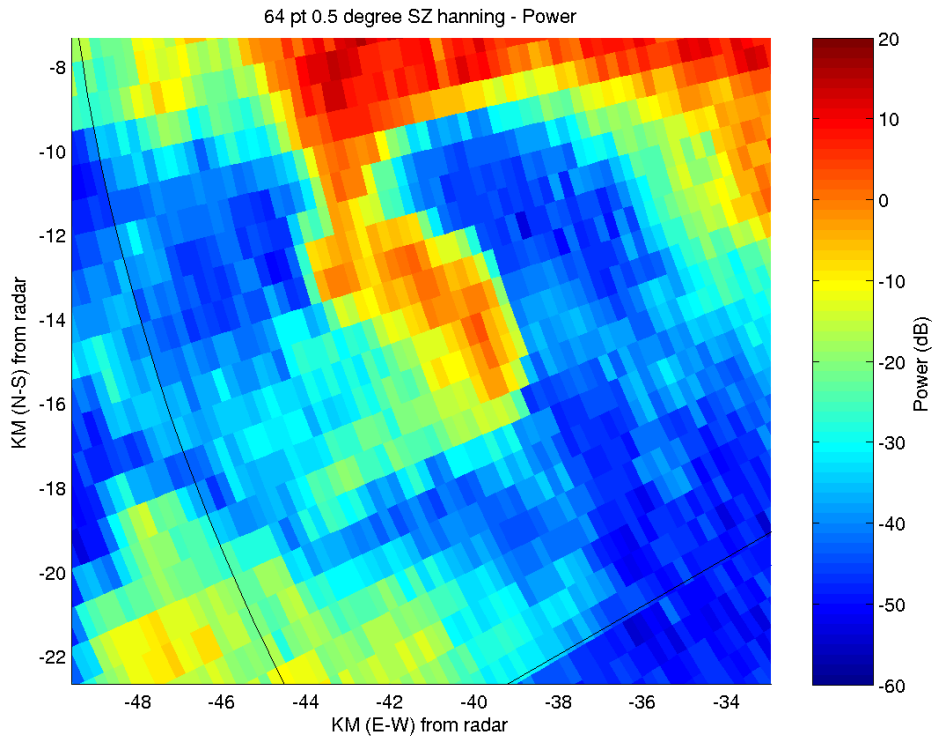


Figure 16: Power calculated over 64 point Hanning window but at 32 point intervals. PPI scans in Fig. 10 are SZ phase coded, overlaid and separated via SZ algorithm.

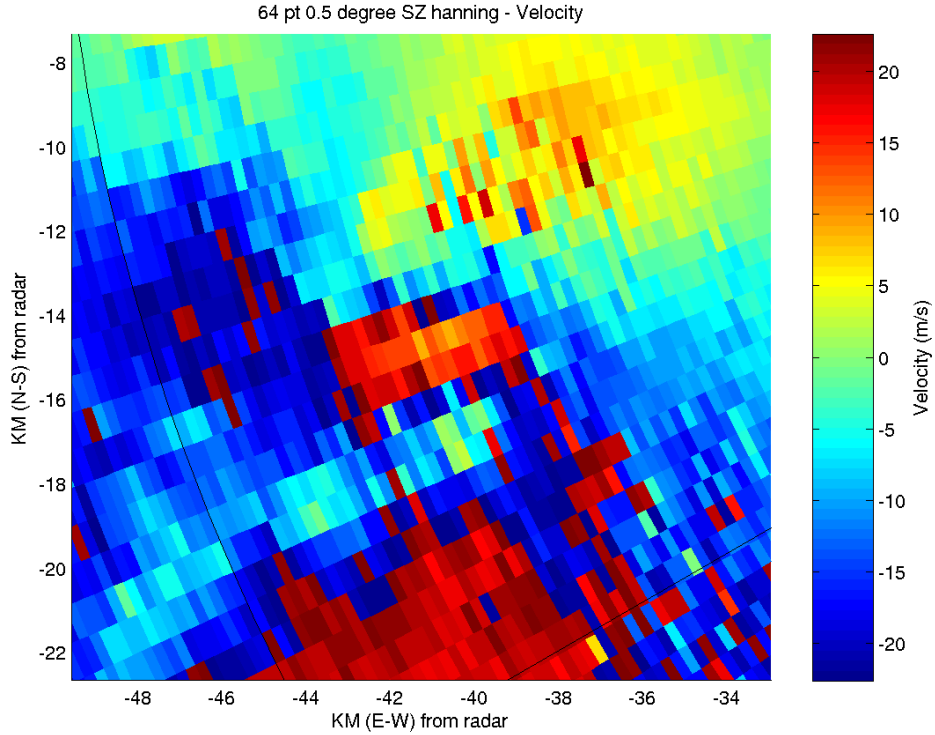


Figure 17: Corresponding velocity plot for Fig. 16.

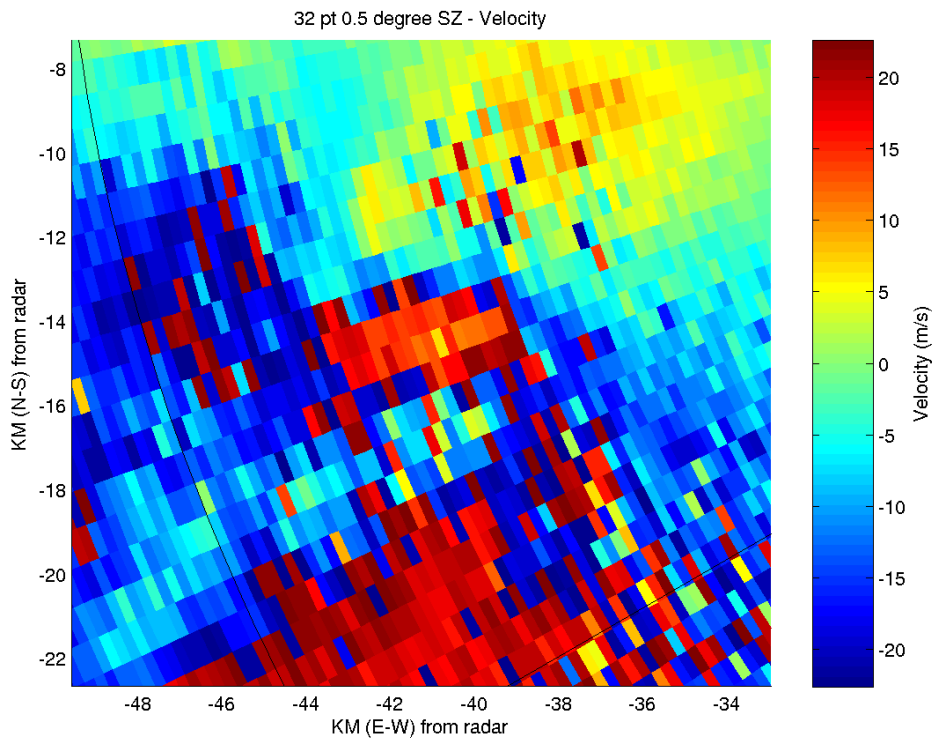


Figure 18: Velocity calculated from a non overlapping 32 point windows using SZ phase coding, i.e., PPI scans in Fig. 10 are SZ phase coded, overlaid and separated via SZ algorithm.